

## Experimental studies of the phase transition in $\text{YbIn}_{1-x}\text{Ag}_x\text{Cu}_4$

A. L. Cornelius\* and J. M. Lawrence  
*University of California, Irvine, California 92697*

J. L. Sarrao\* and Z. Fisk  
*Florida State University, Tallahassee, Florida 32306*

M. F. Hundley, G. H. Kwei, and J. D. Thompson  
*Los Alamos National Laboratory, Los Alamos, New Mexico 87545*

C. H. Booth and F. Bridges  
*University of California, Santa Cruz, California 95064*

(Received 7 April 1997)

We report measurements of the low-temperature specific-heat coefficient  $\gamma=C_p(T)/T$ , cell volume  $V(T)$ , Hall coefficient  $R_H(T)$ , and valence  $z=2+n_f$  [where the Yb hole occupation  $n_f(T)$  was determined from Yb- $L_3$  x-ray absorption] of single crystals of  $\text{YbIn}_{1-x}\text{Ag}_x\text{Cu}_4$ . Alloying  $\text{YbInCu}_4$  with Ag increases the temperature  $T_s(x)$  of the first-order isomorphous phase transition and causes it to terminate at a critical point at  $x_c=0.195$  and  $T_c=77$  K. The variation of  $V(T)$  near the critical point is well described by a mean-field equation of state. The phase transition involves a large change in the Kondo temperature, and the transition temperatures  $T_s(x)$  are of order of the Kondo temperatures  $T_K^+(x)$  of the high-temperature state. The cell volume is found to vary proportionally to  $1-n_f(T)$ . At low temperatures, well away from the transition, the Wilson ratio of the susceptibility  $\chi(0)$  and specific heat coefficient  $\gamma$  falls within 20% of the value predicted for a Kondo impurity, and  $1-n_f(0)$  and  $\chi(0)$  are roughly proportional as predicted from the Anderson model. The temperature dependence  $n_f(T)$  for temperatures away from the phase transition also fits the predictions of the Kondo model. The small volume discontinuity  $\Delta V/V_0$  observed at  $T_s$  suggests that the phase transition is not due to a Kondo volume collapse. The large Hall coefficients  $R_H(T)$  observed for  $x<x_c$  and  $T>T_s(x)$  suggest instead that a low carrier density in the high-temperature state plays a key role in the phase transition. [S0163-1829(97)08436-1]

### INTRODUCTION

$\text{YbInCu}_4$  has a phase transition<sup>1-3</sup> at  $T_s=40$  K that is similar to the "isomorphous"  $\alpha$ - $\gamma$  transition in Ce metal.<sup>4</sup> The density changes (by 0.5%) at the transition<sup>3</sup> with no change<sup>1-3,5</sup> in the crystal symmetry (cubic  $C15b$  structure<sup>2</sup>). In the high-temperature state the Yb ion is nearly trivalent,<sup>1</sup> the susceptibility<sup>1</sup> indicates Yb-4*f* local moment paramagnetism, and the spin dynamics<sup>6</sup> are as predicted for a Kondo impurity with a small characteristic temperature ( $T_K \sim 25$  K). In the low temperature state the Yb ion is mixed valent ( $z \approx 2.8$ ), the susceptibility is that of an enhanced Pauli paramagnet, and the spin dynamics are those of a Kondo impurity with large characteristic energy ( $T_K \sim 500$  K).

$\text{YbInCu}_4$  offers a number of advantages over Ce for studying such an isomorphous phase transition, not the least being that single crystals are available.<sup>7</sup> We have shown<sup>5</sup> that our flux-grown crystals are more highly ordered than polycrystal counterparts, and we have begun a study of the properties of this compound and its alloys, in particular  $\text{YbIn}_{1-x}\text{Ag}_x\text{Cu}_4$ .<sup>7</sup> Using the susceptibility  $\chi(T)$ , we have estimated the variation of the Kondo temperature for different values of alloy concentration  $x$  and temperature  $T$ , and we have shown that there is a critical point for the isomorphous transition in the  $x-T$  plane near  $x_c \approx 0.20$  and  $T_c \approx 80$  K.

In this paper we report studies of the volume thermal expansion  $\beta(T)$ , the low temperature specific heat  $C_p(T)$ , the Hall coefficient  $R_H(T)$  and the 4*f* hole occupation  $n_f(T)$  (as measured by  $L_3$  x-ray absorption) of  $\text{YbIn}_{1-x}\text{Ag}_x\text{Cu}_4$ . Well away from the phase boundary, these properties and the susceptibility interrelate as predicted for a Kondo impurity, and the cell volume varies proportionally to  $1-n_f$ . Near the critical point, the phase transition can be well described by an equation of state similar to that reported<sup>8</sup> for  $\text{Ce}_{1-x}\text{Th}_x$  alloys. In addition, we confirm directly the assumption made in the older study that the order parameter is the 4*f* occupation number  $n_f$  and that the phase transition temperature  $T_s(x)$  corresponds approximately to the Kondo temperature  $T_K^+(x)$  of the high temperature state. Despite the similarities to the Ce  $\alpha$ - $\gamma$  transition, we will argue that the isomorphous transition is not due to a Kondo volume collapse<sup>9</sup> but is connected with a low carrier density [anomalously large  $R_H(T)$ ] observed in the high temperature state of  $\text{YbInCu}_4$ .

### EXPERIMENTAL DETAILS

The samples were single crystals grown in  $\text{In}_{1-x}\text{Ag}_x\text{Cu}$  flux, as reported earlier.<sup>7</sup> A thermal relaxation method<sup>10</sup> was used to measure the specific heat of small ( $\sim 10$ – $30$  mg) samples. The thermal expansion was measured by capacitive dilatometry; samples with dimensions a few mm on a side

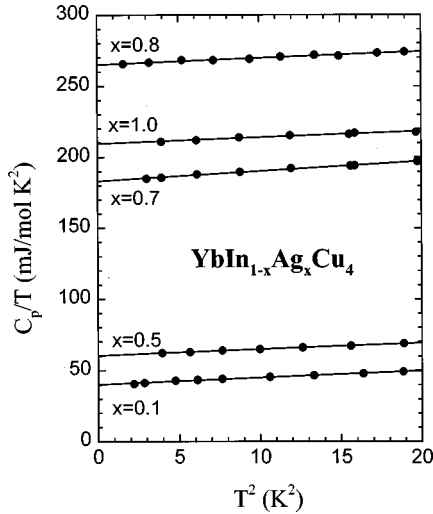


FIG. 1. The low-temperature specific heat  $C_p(T)$  of  $\text{YbIn}_{1-x}\text{Ag}_x\text{Cu}_4$  plotted as  $C_p(T)/T$  versus the square of the temperature for several values of alloy concentration  $x$ . The solid lines are fits to the functional form  $C_p(T) = \gamma T + \delta T^3$ .

were loaded in an oxygen-free high conductivity (OFHC) Cu dilatometry cell<sup>11</sup> and the capacitance was measured using a three-terminal automated capacitance bridge. A sample of high-purity copper was measured to determine background and provide absolute calibration. The experimental resolution for the sample length measurement was  $\sim 0.1 \text{ \AA}$ . The Hall voltage was measured in fields of  $\pm 1 \text{ T}$  for samples of typical dimension  $0.5 \times 2 \times 5 \text{ mm}$  using an LR400 ac resistance bridge. Any small misalignment voltage was compensated electronically and the magnetoresistance was canceled by reversing the polarity of the field. For fields less than  $1 \text{ T}$  the signal was linear in applied field. The magnetic susceptibility results reported below were taken from the same experiments (which used a SQUID magnetometer) reported earlier,<sup>7</sup> the susceptibility has been reanalyzed to correct for a small low temperature ‘‘Curie tail.’’ For the  $L_3$  measurement, flux-grown crystals were finely powdered and dusted onto Kapton tape, then loaded in the window of an aluminum holder which itself was mounted in a continuous flow He cryostat. The experiments were performed in the transmission mode on Beam Line 2-3 at the Stanford Synchrotron Radiation Laboratory (SSRL) utilizing a Si(220) monochromator, detuned 50% to avoid harmonic contamination, and standard ionization detectors. For energy calibration, we simultaneously measured a Cu foil standard. We subtracted a linear background, determined in a wide interval of energy below the absorption edge, from the data and scaled the average absorption in the extended x-ray-absorption fine-structure (EXAFS) region to unity.

## RESULTS AND ANALYSIS

The low-temperature specific heat of representative alloys is shown in Fig. 1. We fit the data to the form  $C_p(T) = \gamma T + \delta T^3$  in the temperature range  $0 < T^2 < 20 \text{ K}^2$ . All samples had values of  $\delta \approx 0.49 \text{ mJ/mol K}^4$ , which corresponds to a Debye temperature  $\theta_D = 288 \text{ K}$ . For  $x=0$  and  $0.1$  a very small ( $\sim 1\%$ ) lambda anomaly was seen near  $2 \text{ K}$  due to the onset of superconductivity in free In on the sample surface.

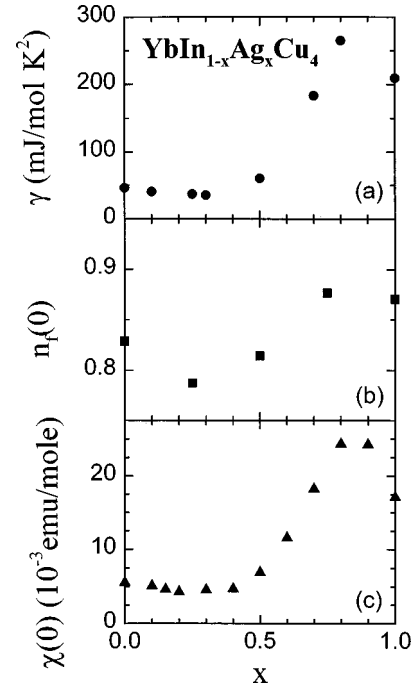


FIG. 2. (a) The electronic coefficients  $\gamma$  of specific heat of  $\text{YbIn}_{1-x}\text{Ag}_x\text{Cu}_4$  determined from the data of Fig. 1, plotted versus alloy concentration  $x$ . (b) The low-temperature hole occupation  $n_f(0)$ , determined from the  $L_3$  data for  $T=15 \text{ K}$  as in Fig. 5, and plotted versus  $x$ . (c) The  $T=0$  susceptibility, obtained from the data of Ref. 7 after correction for a small ‘‘Curie tail,’’ plotted versus  $x$ .

The linear coefficients  $\gamma$  are plotted as a function of alloy concentration in Fig. 2(a) and compared to the values of the ground-state susceptibility  $\chi(0)$ .

The Hall coefficients for a series of alloys as well as for  $\text{LuInCu}_4$  and  $\text{LuAgCu}_4$  are shown in Fig. 3. The solid lines represent least-square fits to the equation

$$R_H(T) = R_0(1 + \varepsilon T) + \eta(g\mu_B/k_B)(\chi(T)/C)\rho(T). \quad (1)$$

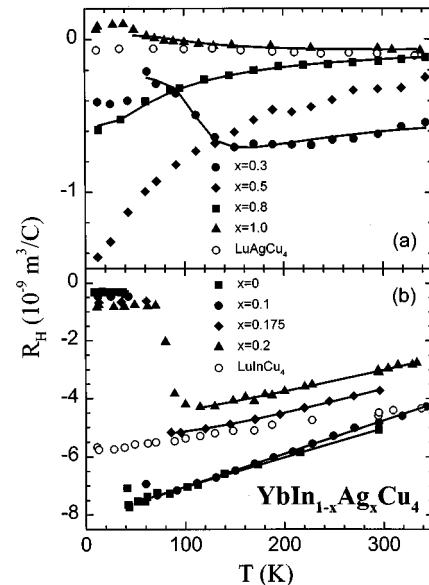


FIG. 3. The Hall coefficient  $R_H(T)$  for  $\text{YbIn}_{1-x}\text{Ag}_x\text{Cu}_4$  and for  $\text{LuAgCu}_4$  and  $\text{LuInCu}_4$ . Note the change of scale between (a) and (b). The solid lines are fits to Eq. (1).

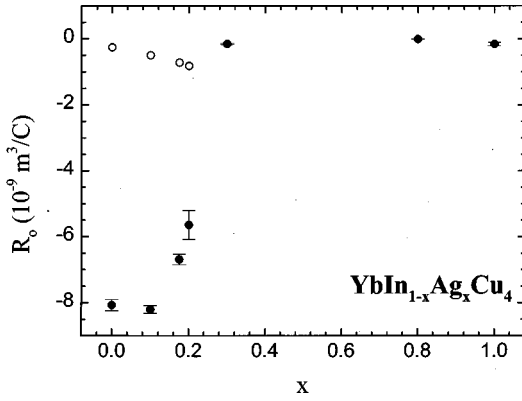


FIG. 4. The normal Hall constant  $R_0$  obtained from fits of Eq. (1) to the data of Fig. 3. For  $x=0-0.2$  the solid circles represent values of  $R_0$  obtained in the high-temperature state, whereas the open circles represent the values obtained in the low-temperature state. If the carrier density obeys  $R_0=1/ne$ , then the carrier density is anomalously low for  $T>T_s(x)$  when  $x\leq x_c\approx 0.2$ .

The first term represents the ordinary Hall effect; the constants  $\epsilon$  are of order  $-(0.001-0.003) \text{ K}^{-1}$  for all  $x$ , comparable to the value  $-0.001 \text{ K}^{-1}$  found for  $\text{LuInCu}_4$ . The second term represents skew scattering<sup>12</sup> of the conduction electrons from Kondo impurities, where  $C=2.582 \text{ emu K/mol}$  and  $g=8/7$  are the Yb  $J=7/2$  free ion Curie constant and Landé factors, respectively, and  $\rho(T)$  is the resistivity (taken from Ref. 7). According to theory<sup>12</sup> the dimensionless constant  $\eta$  should approximately equal  $\sin \delta_2$ , where  $\delta_2$  is the phase shift for nonresonant scattering (e.g., potential scattering in the  $d$  channel). This phase shift should not be large; values as large as 0.2 are deemed unrealistic.<sup>12</sup> By this criterion, the values we obtain for  $\eta$  from the fits for  $\text{YbInCu}_4$ ,  $\text{YbIn}_{0.9}\text{Ag}_{0.1}\text{Cu}_4$ , and  $\text{YbAgCu}_4$  ( $-0.07$ ,  $+0.08$ , and  $+0.07$ ) are quite reasonable but the larger values observed for intermediate  $x$  (0.8, 0.5,  $-1.1$ , and  $-0.6$  for  $x=0.175$ , 0.2, 0.3, and 0.8, respectively) are too large. We have not corrected the resistivity for background scattering such as electron-phonon scattering; the resulting smaller resistivity would require an even larger value of  $\eta$  to be used in the fits. For  $x\leq 0.2$ , the major temperature dependence comes from the normal term, and is comparable to the temperature dependence for  $\text{LuInCu}_4$ , while for  $x=0.5$ , the factor of 6 change in the Hall coefficient is much too large to be explained by skew scattering, since the resistivity and susceptibility for this compound<sup>7</sup> vary only by 10% over the whole temperature range. Hence the large values of  $\eta$  observed for  $0.175\leq x\leq 0.8$  may arise from incorrect estimation of the normal Hall contribution. Despite these reservations, the estimates of  $R_0$  obtained from these fits, which are plotted in Fig. 4, are essentially correct because any errors in  $R_0$  will be modest. In the simplest picture, one can relate  $R_0$  to the carrier concentration by  $R_0=1/ne$ , where  $n$  is the carrier concentration and  $e$  is charge of the carrier. For  $x=0$ ,  $n$  changes from 0.07 carriers per formula unit for  $T>T_s$  to 2.2 carriers per formula unit for  $T<T_s$ . Though there may be some error in  $R_0$ , the important point is that there is a large change in  $R_0$  between the high- and low-temperature state for  $x\leq x_c\approx 0.20$  and between the high-temperature states for  $x<0.2$  and  $x>0.2$ . A more thorough multiband analysis would not change this conclusion.

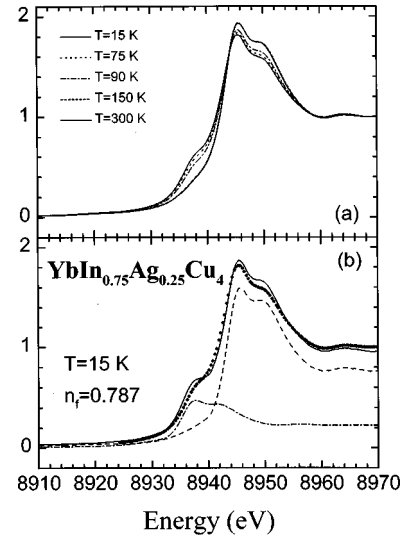


FIG. 5. (a) The  $L_3$  spectra of  $\text{YbIn}_{0.75}\text{Ag}_{0.25}\text{Cu}_4$  at several temperatures plotted versus photon energy. A linear background has been subtracted from the data, and the spectra are normalized to a step height of unity in the EXAFS region. (b) An example of the fitting procedure for extracting the  $4f$  hole occupation  $n_f$  and valence  $z=2+n_f$  from the data (squares) for  $\text{YbIn}_{0.75}\text{Ag}_{0.25}\text{Cu}_4$  at  $T=15 \text{ K}$ . The dashed and dotted lines are replicas of the absorption line shape of  $\text{LuInCu}_4$ , which is chosen to represent integral-valent absorption. The dashed (dotted) line is shifted in energy to coincide with the absorption edge for trivalent (divalent) Yb. The solid line is a weighted sum of the two replicas, with weighting factors  $n_f$  (trivalent) and  $1-n_f$  (divalent) chosen to give the best fit. (See text for details.)

The  $L_3$  x-ray-absorption spectra for  $\text{YbIn}_{0.75}\text{Ag}_{0.25}\text{Cu}_4$  are shown in Fig. 5(a). A shoulder near 8937 eV, which represents absorption by divalent Yb, appears as the temperature is lowered, and the “white line” at 8945 eV and secondary peak at 8950 eV, which represent absorption by trivalent Yb, decrease with temperature. Spectra for other values of  $x$  are similar, but show differing degrees of temperature dependence. To determine the Yb valence  $z=2+n_f$  (where  $n_f$  is the occupation number of holes in the  $4f$  shell) from these spectra, we adopt a standard procedure (e.g., Ref. 1). We determine the energy dependence for trivalent absorption by measuring the  $L_3$  absorption spectra of  $\text{LuInCu}_4$  and  $\text{LuAgCu}_4$ ; these had essentially identical absorption spectra that were independent of temperature (which also establishes that any temperature dependence observed in the Yb compounds is due to change of the valence). We smoothed the Lu spectrum in the region below its absorption edge at 9240 eV to account for the fact that the Lu  $L_3$  absorption is superimposed on the EXAFS from the Cu  $K\alpha$  edge at 9000 eV (which is not the case for the Yb  $L_3$  edge at 8940 eV); also, we adjusted the Lu spectra so that the slope at an energy 20 eV below the “white line” agreed with the slope of the spectra of the Yb compounds at 8920 eV, which is 20 eV below the white line for the trivalent component. This gave our assumed form for the trivalent spectrum. We then fit the Yb spectrum to the sum of two replicas of this trivalent spectrum, one representing trivalent absorption with a white line centered at 8945 eV, and the other representing divalent absorption with a white line centered at 8937 eV. A representative fit, including the Yb spectrum, as well as the divalent

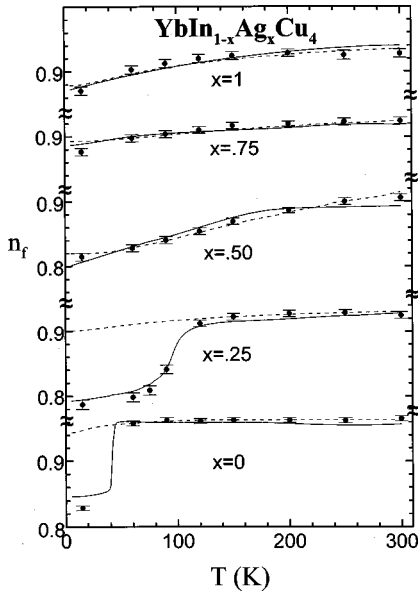


FIG. 6. The 4f occupation numbers  $n_f(T)$  of  $\text{YbIn}_{1-x}\text{Ag}_x\text{Cu}_4$  plotted versus temperature for five values of alloy concentration  $x$ . The solid symbols are determined from  $L_3$  data as in Fig. 5. The solid lines are determined from the anomalous contribution  $\delta V(T)/V_0$  to the cell volume (see Fig. 7), using Eq. (2). The dashed lines are theoretical calculations using the Anderson model (see text for details).

and trivalent replicas, is shown in Fig. 5(b). The 4f hole occupation  $n_f$  was then determined from the relative weights of the divalent and trivalent contributions. The ground-state values of  $n_f(0)$  are plotted in Fig. 2(b), and the temperature dependence  $n_f(T)$  for different alloy concentrations  $x$  is plotted as solid circles in Fig. 6.

The assumptions that the divalent line shape is a replica of the trivalent and that the latter can be taken from the Lu analog compound are not expected to be strictly valid, and to the extent that they are not valid, we expect systematic error in our estimates of  $n_f$ . As shown in Fig. 6 and discussed further below, the values of  $n_f(T)$  deduced from the  $L_3$  measurement correspond to those deduced from the thermal expansion and from the theory of an Anderson impurity; this lends support to the procedure.

As a representative example of the measurement of sample volume using the capacitive dilatometer, we show  $V(T)/V_0$  (where  $V_0$  is the volume at 300 K) for  $\text{YbIn}_{0.75}\text{Ag}_{0.25}\text{Cu}_4$  in Fig. 7. Also included are the data for the trivalent compound  $\text{LuAgCu}_4$ . This compound has nearly the same thermal expansion as  $\text{LuInCu}_4$ , and hence we assume that it equals the thermal expansion of trivalent Yb for all alloy concentrations  $x$ . Subtracting this from the Yb data, we arrive at the anomalous contribution  $\delta V(T)/V_0$  to the volume which arises from the change in valence with temperature. We calculate  $n_f$  from the formula

$$1 - n_f(T) = [\delta V(T)/V_0] / [(V_2 - V_3)/V_0], \quad (2)$$

where  $V_2$  and  $V_3$  are the ground-state volumes of the hypothetical divalent and trivalent Yb compounds. Since the thermal expansions are small,  $V_3$  and  $V_0$  are equal to within a few tenths of a percent, so  $(V_2 - V_3)/V_0 \approx [(V_2/V_3) - 1]$ ; we use the value  $V_2/V_3 = 1.046$  suggested by earlier

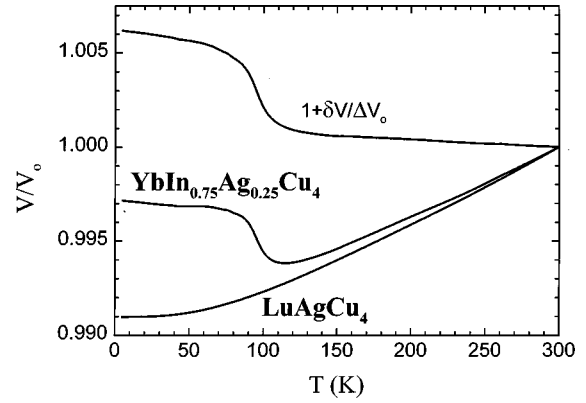


FIG. 7. The cell volume  $V(T)/V_0$  (where  $V_0$  is the room-temperature volume) for  $\text{YbIn}_{0.75}\text{Ag}_{0.25}\text{Cu}_4$  and  $\text{LuAgCu}_4$  plotted versus the temperature. The anomalous contribution to the cell volume  $\delta V(T)/V_0$  is the difference between these two curves.

authors.<sup>13</sup> In the analysis it is necessary to add a constant to the room-temperature value of  $\delta V(T)/V_0 = [V(\text{Yb})/V_0 - V(\text{Lu})/V_0]$  (which would otherwise be zero) so that Eq. (2) gives the correct  $L_3$  valence at the room temperature. The resulting  $n_f(T)$  curves for several values of  $x$  are plotted in Fig. 6 along with the values determined from the  $L_3$  experiments.

From Fig. 6 it can be seen that the discontinuity observed at the first order transition ( $T_s = 40$  K) in  $\text{YbInCu}_4$  becomes broad and S-shaped for  $x = 0.25$ . This means that in the  $x$ - $T$  plane, the line of first-order transitions  $T_s(x)$  terminates at a critical point at some  $x_c < 0.25$  and that for larger  $x$  the transitions are analytic. In Fig. 8 we plot  $\Delta V(T)/V_0(x)$  for concentrations  $x < 0.3$  and for a temperature interval  $\pm 30$  K about the temperature  $T_s(x)$  of the isostructural transition. Here  $\Delta V(T) = V(T) - V_0(x)$ ,  $V_0(x) = V(T_s(x))$ , and  $T_s(x)$  was chosen as the temperature of maximum slope (the data shown were all taken on warming the sample); the values of  $T_s(x)$  are shown in Fig. 9. To locate the critical point, we

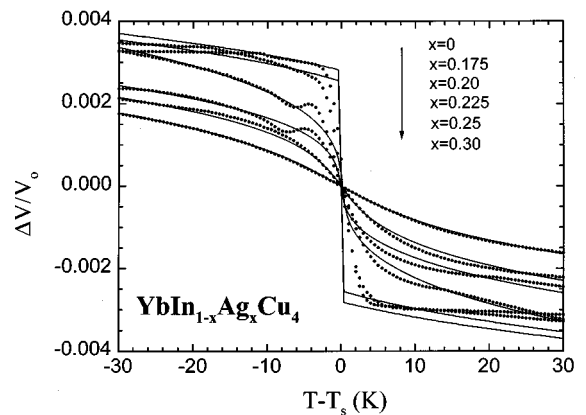


FIG. 8. A plot of  $\Delta V(T)/V_0(x)$  versus temperature in an interval  $\pm 30$  K about the temperature  $T_s(x)$  of the isostructural transition for several concentrations  $x \leq 0.3$  of  $\text{YbIn}_{1-x}\text{Ag}_x\text{Cu}_4$ . Here  $\Delta V(T) = V(T) - V_0(x)$ , where  $V_0(x) = V(T_s(x))$ . The solid lines represent predictions of the mean-field equation of state [Eq. (3)]. The curves for  $x < 0.20$  represent first-order transitions, for  $x > 0.20$ , analytic (“supercritical”) transitions, and for  $x = 0.20$  the curve represents a critical transition at  $x \approx x_c$ .

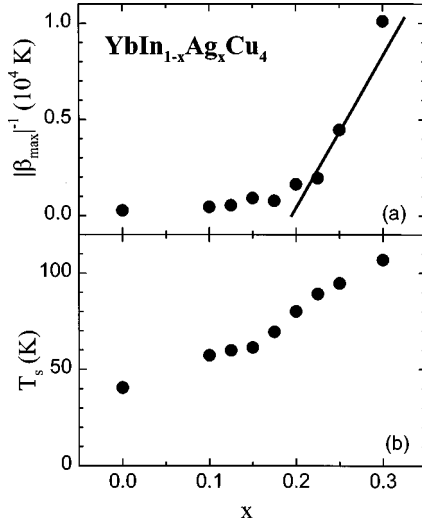


FIG. 9. (a) The inverse of the maximum value of the volume thermal expansion coefficient  $\beta_{\max}$  plotted versus alloy concentration  $x$  for  $\text{YbIn}_{1-x}\text{Ag}_x\text{Cu}_4$ . By Eq. (4) the maximum value  $\beta_{\max}$  for any  $x > x_c$  occurs when  $T = T_s(x)$ ; furthermore  $\beta_{\max}^{-1}$  extrapolates to zero at  $x = x_c$ . We deduce that  $x_c \approx 0.20$ ; for  $x \leq 0.20$  there is a residual value of  $\beta_{\max}^{-1}$  due to inhomogeneity rounding of the first-order transitions. The solid line represents the prediction of Eq. (4) using the same parameters as in Fig. 8. (b) The temperatures  $T_s(x)$  of the isostructural transitions, determined from the temperature of the maximum value  $\beta_{\max}$  of volume thermal expansion, and plotted versus  $x$  (solid circles).

have fit the data to a mean-field equation of state similar to that used in the past<sup>8</sup> to describe the behavior of the  $\alpha$ - $\gamma$  transition in  $\text{Ce}_{1-x}\text{Th}_x$  alloys:

$$a(\Delta V/V_0)^3 + b\Delta x(\Delta V/V_0) = \Delta T - c\Delta x. \quad (3)$$

In this expression  $\Delta x = x - x_c$  and  $\Delta T = T - T_c$ , where  $T_c = T_s(x_c)$ . To determine  $x_c$  we note that the volume thermal expansion arising from the equation of state is

$$\beta^{-1} = 3a(\Delta V/V_0)^2 + b\Delta x. \quad (4)$$

For any  $x > x_c$ , the maximum value  $\beta_{\max}$  occurs at  $T = T_s(x) = T_c + c\Delta x$  and  $\beta_{\max}^{-1} = b\Delta x$ , which extrapolates to zero at  $x = x_c$ . We plot this in Fig. 9, where it can be seen that  $x_c \approx 0.20$  for which  $T_c \approx 80$  K. [For  $x < x_c$ , the first-order transitions are not perfectly sharp, due to inhomogeneity rounding; hence they have a finite but large slope at  $T_s(x)$ .] These values of  $x_c$  and  $T_c$  are in good agreement with those determined earlier from the susceptibility.<sup>7</sup> We then fit the data in Fig. 8 to Eq. (3); the fits are shown as solid lines, and the values of parameters are  $T_c = 77 \pm 2$  K,  $x_c = 0.195 \pm 0.005$ ,  $a = [(0.96 \pm 0.21) + (16.7 \pm 2.0)\Delta x] \times 10^9$  K,  $b = (7.9 \pm 0.8) \times 10^4$  K, and  $c = 211 \pm 9$  K. The solid line in Fig. 9 represents the prediction for  $\beta_{\max}^{-1}(x)$  using these values. Although inhomogeneity rounding is apparent in Figs. 8 and 9, and there appear to be small secondary transitions for  $x = 0.2$  and  $0.225$  (again, probably due to alloy inhomogeneity), the equation of state gives a reasonable overall description of the data in the vicinity of the critical point.

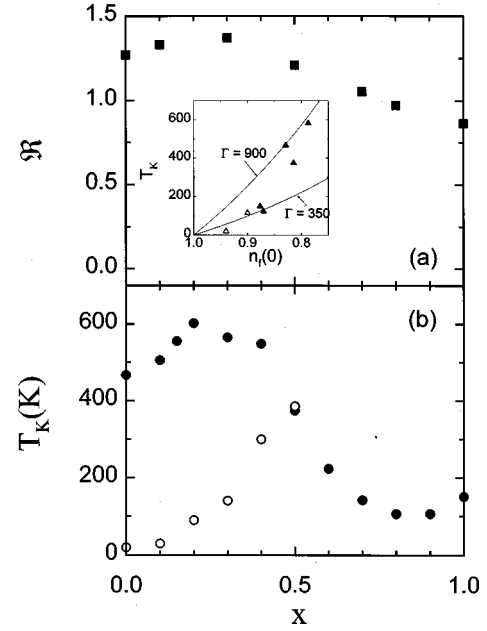


FIG. 10. (a) The Wilson ratio of susceptibility and specific heat  $\mathcal{R} = (\pi^2 R/3C)(\chi/\gamma)$  plotted versus alloy parameter  $x$  for  $\text{YbIn}_{1-x}\text{Ag}_x\text{Cu}_4$ . The prediction of the Kondo model for a  $J = 7/2$  moment is  $\mathcal{R} = 8/7$ . (b) The Kondo temperatures  $T_K^-$  of the low-temperature state, taken as  $T_K^- = C/\chi(0)$  (solid circles), and  $T_K^+$  of the high-temperature state, obtained by fitting the high-temperature susceptibility to the Kondo model as in Ref. 7 (open circles), plotted versus  $x$ . Inset: the low-temperature Kondo temperature  $T_K^-$  plotted versus the low-temperature  $4f$  hole occupation  $n_f(0)$ . The solid lines represent the predictions of Eq. (4) for  $\Gamma = 350$  and  $900$  K.

## DISCUSSION

We first discuss the behavior in the region away from the phase boundary  $T_s(x)$ . Examination of Fig. 2 shows that at low temperature the quantities  $\chi(0)$ ,  $\gamma$ , and  $n_f(0)$  all vary proportionally. In fact, all three quantities reach a maximum value for  $x \approx 0.8$  corresponding to the low-temperature Kondo temperature having its minimum value for the alloy series at this concentration. In Fig. 10(a) we show the Wilson ratio, i.e., the normalized ratio  $\mathcal{R} = (\pi^2 R/3C)(\chi/\gamma)$ , where  $R$  is the gas constant and  $C$  is the free ion Curie constant for  $J = 7/2$  Yb. In the Kondo limit of the impurity Anderson model,<sup>14</sup> this ratio should have the value  $\mathcal{R} = (2J + 1)/2J = 8/7$ . The data lie within 20% of this value for all  $x$ . In evaluating  $\mathcal{R}$  we have not corrected either  $\chi(0)$  or  $\gamma$  for background contributions, which are best estimated by measuring these quantities for the counterpart  $\text{LuIn}_{1-x}\text{Ag}_x\text{Cu}_4$  compounds; however,  $\chi(0)$  is known<sup>15</sup> to be small ( $-0.5 \times 10^{-3}$  emu/mol) in  $\text{LuInCu}_4$ , and we have measured an even smaller value ( $0.05 \times 10^{-3}$  emu/mol) for  $\text{LuIn}_{0.3}\text{Ag}_{0.7}\text{Cu}_4$ . Hence this correction should have little effect on  $\mathcal{R}$ . On the other hand, for  $\text{LuIn}_{0.3}\text{Ag}_{0.7}\text{Cu}_4$  and  $\text{LuAgCu}_4$  we measure  $\gamma = 7.0$  and  $10.1$  mJ/mol K<sup>2</sup>, respectively; assuming that this is the background contribution, correcting for this gives a 4–5 % increase in  $\mathcal{R}$  to 1.10 and 0.91 for the two Yb compounds, respectively. If the correction required for small  $x$  has a comparable value (10 mJ/mol K<sup>2</sup>), the resulting increase in  $\mathcal{R}$  would be even larger, e.g., to a value 1.62 for  $\text{YbInCu}_4$ .

In the Kondo impurity limit it is approximately true<sup>14</sup> that the Kondo temperature  $T_K$  is related to the susceptibility by  $\chi(0) = C/T_K$  and to the hybridization strength  $\Gamma = V_{kf}^2 \rho(\epsilon_F)$  [where  $V_{kf}$  is the  $4f$  conduction electron hybridization matrix element and  $\rho(\epsilon_F)$  the conduction electron density of states at the Fermi level] by

$$T_K = [(2J+1)\Gamma/\pi] \{ [1 - n_f(0)]/n_f(0) \}. \quad (5)$$

In Fig. 10(b) we plot the Kondo temperature of the low-temperature phase  $T_K^+ = C/\chi(0)$  as a function of  $x$ , and in the inset to Fig. 10(a) as a function of  $n_f(0)$ , the latter determined from the  $L_3$  results (Fig. 2). The values of  $T_K^-$  increase as  $1 - n_f(0)$  increases, but they cannot be fit by Eq. (5) assuming a constant value of  $\Gamma$  for all values of  $x$ . If we take Eq. (5) literally, then the inset suggests that  $\Gamma$  decreases from a value of order 900 K (0.078 eV) for the low-temperature state at  $x=0$  and 0.25 to a value of order 350 K (0.029 eV) for  $x=0.75$  and 1; the crossover data point occurs at  $x=0.5$ . The open triangles in the inset represent estimates of  $T_K^+$  (obtained by fitting the high-temperature susceptibility to the predictions of the Kondo model as in Ref. 7) and  $n_f(0)$  for the high-temperature state for  $x=0$  and 0.25; these suggest even smaller values of  $\Gamma$ .

In Fig. 6 we compare the experimental results for the temperature dependence of the occupation number  $n_f(T)$  to the predictions<sup>14</sup> of the Anderson model. We have used theoretical results for  $J=5/2$  since results for  $J=7/2$  have not been reported; we assume that differences between the predictions for the two cases are small and of the order of experimental error. The theoretical curves obey a scaling relation and are fixed by two parameters,  $n_f(0)$  and  $T_K$ . For  $x \geq 0.5$ , we use the values for  $n_f(0)$  and  $T_K^- = C/\chi(0)$  determined from Fig. 2; for  $x=0$  and 0.25, we use the high-temperature value of  $T_K^+$  and choose  $n_f(0)$  to give a good fit to the high-temperature data. The theory represents the data reasonably well at all temperatures for  $x \geq 0.5$ ; for smaller  $x$  (where the phase transition causes a change in  $T_K$  with temperature, as discussed below), the theory fits the data well at temperatures sufficiently greater than  $T_s(x)$ .

Hence the single impurity Anderson model is adequate to interrelate the ground-state quantities  $\chi(0)$ ,  $\gamma$ , and  $n_f(0)$  and to describe the temperature dependence of  $n_f(T)$ . It has also been shown<sup>6</sup> to describe the magnetic inelastic neutron scattering spectrum of YbInCu<sub>4</sub>. On the other hand, the Yb sublattice is periodic in these compounds and the periodicity is expected<sup>14</sup> to give rise to ‘‘coherence’’ at low temperatures. A possible manifestation of coherence in our data is the observed deviation of the Wilson ratio from the value 8/7 expected for a Kondo impurity. This could occur if the ground-state  $4f$  spectrum is that of a narrow  $4f$  band with structure different from the nearly Lorentzian resonance spectrum expected<sup>14</sup> for an Anderson impurity.

The Anderson model does not include coupling to the cell volume, which must be added as an additional assumption. The oldest assumption<sup>4</sup> is that, because the divalent Yb ion is larger than the trivalent ion, the cell volume  $\delta V(T)/V_0$  should vary proportionally to  $n_f$ , i.e., Eq. (2) should give an adequate description of the relationship between these quantities. Figure 6 shows that for most  $x$  and  $T$  the cell volume

$\delta V(T)/V_0$  does indeed vary proportionally to  $n_f$ , as determined from the  $L_3$  experiments.

We now turn to the phase transition. Figure 8 shows that the data are well fit by a mean-field equation of state [Eq. (3)] that itself follows from a Landau free energy of the form,

$$\Phi = (a/4)(\Delta V/V_0)^4 + (b\Delta x/2)(\Delta V/V_0)^2 - (\Delta T - c\Delta x)(\Delta V/V_0). \quad (6)$$

This is of the same form as has been shown to be valid for the  $\alpha$ - $\gamma$  transition in Ce<sub>1-x</sub>Th<sub>x</sub> alloys,<sup>8</sup> where it was pointed out that it is analogous to the free energy of a ferromagnet in a magnetic field, but with the replacements  $\Delta T = T - T_c \rightarrow \Delta x = x - x_c$  and  $H \rightarrow T - T_s(x) = \Delta T - c\Delta x$ . We note further that in the older work it was assumed that in the vicinity of the critical point the volume change  $\Delta V(T)/V_0$  varies proportionally to  $n_f(T)$ . Our  $L_3$  results allow us to confirm this assumption (see especially the case  $x=0.25$  in Fig. 6). This means that the order parameter can be taken to be the  $4f$  occupation number  $n_f$ .

The phase transition can be viewed very generally in the following way. In the absence of interactions between the  $4f$  electrons, the system obeys the energetics of the single-ion Anderson model. The occupation number (order parameter)  $n_f$  saturates to unity at high temperature in order to lower the free energy by taking advantage of the spin entropy available when the Yb  $4f$  electron localizes in the trivalent state. This creates the analogy between temperature in the isomorphous transition and magnetic field in the ferromagnetic transition (where the order parameter saturates at high magnetic field). Some form of interaction coupling the values of  $n_f$  on different sites creates the highly nonlinear dependence of the order parameter  $n_f$  on  $T$  that drives the phase transition.

In the case of a mean-field ferromagnet, the strength of the interactions is measured by the molecular field constant  $\lambda = T_c/C$  (where  $C$  is the Curie constant) and is reflected in the term  $(b/2)(T - T_c)M^2$  in the free energy. By analogy the strength of the interactions for the isomorphous transition is measured by  $x_c$ , or rather by the ratio  $bx_c/a$ . (More precisely, the value of  $x_c$  measures the efficiency of the solute in weakening the interactions.) A study of how the critical concentration  $x_c$  depends on the solute  $M$  in YbIn<sub>1-x</sub>M<sub>x</sub>Cu<sub>4</sub> would thus give secondary information on the physical chemistry of the interactions.

As can be seen in the plot (Fig. 10b) of the Kondo temperatures  $T_K^-$  and  $T_K^+$  of the low and high temperature states, there is a large change in the Kondo temperature at the phase transition. This has been directly observed<sup>6</sup> in neutron scattering experiments. This decrease in  $T_K$  above  $T_s$  is connected with the large decrease in hybridization parameter  $\Gamma$  mentioned above. In addition, the phase transition temperature  $T_s(x)$  is very nearly equal to the Kondo temperature  $T_K^+$  of the high temperature state; this can be seen by comparing Figs. 9 and 10. A similar relationship was observed in Ce<sub>1-x</sub>Th<sub>x</sub> alloys<sup>16</sup> and in  $\gamma$ -Ce,<sup>17</sup> where the Curie-Weiss  $\theta$  (which is an estimate of  $T_K$ ) satisfies  $\theta(P) = T_s(P)/2$ . The reason for this equality is that the transition occurs when  $n_f$  begins to change rapidly with temperature, and the most

rapid variation of  $n_f(T)$  occurs at temperatures in the vicinity of  $T_K$ . Because the high-temperature state has the smaller Kondo temperature, as the temperature increases to values of order  $T_K^+$  the system can gain spin entropy and hence lower the free energy by transforming to the high-temperature state.

The key question for understanding isomorphous transitions concerns the precise nature of the interactions responsible for the transition. A large change in  $T_K$  is also observed at the Ce  $\alpha$ - $\gamma$  transition, which suggests a similar mechanism for the phase transition. The Kondo volume collapse (KVC) model<sup>9</sup> of the Ce  $\alpha$ - $\gamma$  transition is based on the idea that the isomorphous transition arises from dependence of the  $4f$ -conduction electron hybridization  $\Gamma$  on cell volume. As the temperature is lowered and  $n_f$  decreases, the degree of mixed valence increases causing a decrease in the Ce cell volume; this increases the  $4f$ -conduction electron overlap, and consequently increases  $\Gamma$ , which in turn [by Eq. (5)] increases  $T_K$  and hence decreases  $T/T_K$ . Because  $n_f$  is a monotonically increasing function of  $T/T_K$ , the net effect is that  $n_f$  decreases more rapidly with decreasing temperature than in the absence of the effect. In this model the existence of the transition depends on a large change in Kondo condensation energy ( $\approx k_B T_K$ ) correlated with the large change in cell volume at the phase transition and a substantial volume dependence of the hybridization  $\Gamma$ . Quantitatively, the change in  $T_K$  at the transition satisfies  $\Delta T_K/T_K = -\Omega \Delta V/V_0$ , where  $\Omega = -\partial \ln T_K / \partial \ln V$  is the Gruneisen parameter. The latter can be estimated from the pressure dependence of the Curie-Weiss  $\theta$  parameter ( $\theta \propto T_K$ ) using the formula  $\Omega = B(1/\theta) d\theta/dP$ , where  $B$  is the bulk modulus. Using the measured values for  $\gamma$ -Ce [ $B = 215$  kbar,<sup>18</sup>  $(1/\theta) d\theta/dP = 0.2$  kbar,<sup>17</sup> and  $\Delta V/V_0 \approx -0.2$  (Ref. 17)] gives  $\Omega = 43$  and  $\Delta T_K/T_K = 8.6$ . The observed increase in  $T_K$  at the transition (from 200 K for  $\gamma$ -cerium to 1500 K for  $\alpha$ -cerium<sup>9</sup>) is consistent with this estimate.

Such an analysis for YbInCu<sub>4</sub>, where  $T_K$  increases from a value of order 25 K at high temperature to a value of order 500 K at low temperature (i.e.,  $\Delta T_K/T_K = 20$ ) and where the volume discontinuity is  $\Delta V/V_0 = 0.005$ ,<sup>7</sup> requires a Gruneisen parameter of order 4000 in the high-temperature state. Viewed from the low-temperature state where  $\Delta T_K/T_K = -1$ , the Gruneisen parameter must be 200. These values are unrealistically large. Indeed, we can estimate the Gruneisen parameter in the high-temperature state using the above-mentioned observation that  $T_s \approx T_K^+$  and the observation<sup>19</sup> that for  $P = 10$  kbar,  $T_s$  decreases from 40 to 20 K. Taking the bulk modulus of YbInCu<sub>4</sub> to be  $B = 1100$  kbar,<sup>20</sup> we have  $\Omega = B(1/T_s) dT_s/dP = 55$  (not an unreasonable value for a heavy fermion system) and  $\Delta T_K/T_K = \Omega \Delta V/V_0 = 0.275$ . Such a small volume discontinuity simply cannot generate the large change in  $T_K$  observed at the transition in YbInCu<sub>4</sub>. [As an added point, we note that the thermal expansion of YbInCu<sub>4</sub> in the high-temperature state over the interval 40–300 K is larger than occurs at the transition (Fig. 7). If the Kondo temperature were simply a function of cell volume, as in the Kondo volume collapse model, a large Kondo temperature and substantial mixed valence would be expected at room temperature, which is not observed.]

In summary, the isomorphous phase transition in YbInCu<sub>4</sub> is similar to that occurring in Ce metal in two respects. First, both YbIn<sub>1-x</sub>Ag<sub>x</sub>Cu<sub>4</sub> and Ce<sub>1-x</sub>Th<sub>x</sub> obey a similar mean-field equation of state. This is a very general feature of this class of transitions.<sup>21</sup> Second, in both cases large changes in Kondo temperature are observed at the phase transition, where the phase transition temperature is comparable to the Kondo temperature  $T_K^+$  of the high-temperature state. The system lowers the free energy by taking advantage of the large spin entropy available of  $T > T_K^+$ . The transitions differ, however, in that for Ce, as opposed to YbInCu<sub>4</sub> the large change in  $T_K$  is driven by a large volume change.

A possible clue to the origin of the phase transition can be seen in Fig. 4. The high-temperature Hall coefficients  $R_0$  vary dramatically as a function of the Ag alloying. If it is assumed that the carrier concentration is coupled to the phase transition, then it should be possible to estimate the critical concentration  $x_c$  from  $R_0(x)$  by determining where  $dR_0/dx$  has its maximum value. Using this technique yields  $x_c = 0.2$  in agreement with the value determined from thermal expansion measurements. The large Hall coefficients  $R_0$  observed in the high-temperature state for  $x \leq x_c \approx 0.2$  suggest an anomalously small carrier density in this region of the phase diagram. This low carrier density is also observed in LuInCu<sub>4</sub>, and it has been attributed<sup>22</sup> to semimetallic behavior, where hole and electron pockets with small carrier density (0.04 carriers per formula unit, in reasonable agreement with our experimental value of 0.07) overlap at the Fermi surface. As a result there is a valley with a small density of states  $\rho(\epsilon_F)$  at the Fermi level separating a peak below  $\epsilon_F$  with a large density of hybrid Cu- $s$ ,  $p$ ,  $d$ , Lu- $d$  and In- $p$  states from a peak above  $\epsilon_F$  with a large density of Lu  $d$  states. Assuming that for trivalent Yb the Fermi level will also be in the valley, then  $\Gamma = V_{kf}^2 \rho(\epsilon_F)$  would be small, and therefore  $T_K$  will be small, as observed. In the mixed valent state, electrons must be removed from the conduction band to provide the extra electrons in the Yb  $4f$  shell. If this lowers the Fermi level into the region of the peak in the density of states, then  $\Gamma$  and hence  $T_K$  will increase. This theory agrees well with our experimental observation that the carrier density changes from 0.07 to 2.2 carriers per formula unit at  $T_s$  in YbInCu<sub>4</sub>. If this interpretation is correct, the transition does not require a large volume change, but depends on the ability of the system to gain a large condensation energy ( $\approx k_B T_K$ ) by a small shift in Fermi level and Yb valence.

#### ACKNOWLEDGMENTS

Work at Irvine and Florida State was supported by the NSF through Grants No. DMR-9501528 and No. DMR-9501529. Work by JLS was performed under the auspices of the NHMFL, which is supported by the NSF and the State of Florida under cooperative agreement DMR-9016241. Work at Los Alamos was performed under the auspices of the U.S. DOE. The x-ray-absorption experiments were performed at the Stanford Synchrotron Radiation Laboratory, which is operated by the U.S. DOE, Division of Chemical Sciences, and by the NIH, Biomedical Resource Technology Program, Division of Research Resources.

- \*Present address: Los Alamos National Laboratory, Los Alamos, NM 87545.
- <sup>1</sup>I. Felner *et al.*, Phys. Rev. B **35**, 6956 (1987).
- <sup>2</sup>K. Kojima *et al.*, J. Magn. Magn. Mater. **81**, 267 (1989).
- <sup>3</sup>K. Kojima *et al.*, J. Phys. Soc. Jpn. **59**, 792 (1990).
- <sup>4</sup>J. M. Lawrence, P. S. Riseborough, and R. D. Parks, Rep. Prog. Phys. **44**, 1 (1981).
- <sup>5</sup>J. M. Lawrence *et al.*, Phys. Rev. B **54**, 6011 (1996).
- <sup>6</sup>A. Severing *et al.*, Physica B **163**, 409 (1990); J. M. Lawrence *et al.*, Phys. Rev. B **55**, 14 467 (1997).
- <sup>7</sup>J. L. Sarrao *et al.*, Phys. Rev. B **54**, 12 207 (1996).
- <sup>8</sup>J. M. Lawrence, M. C. Croft, and R. D. Parks, in *Valence Instabilities and Related Narrow Band Phenomena*, edited by R. D. Parks (Plenum, New York, 1977), p. 35.
- <sup>9</sup>J. W. Allen and R. M. Martin, Phys. Rev. Lett. **49**, 1106 (1982); J. W. Allen and L. Z. Liu, Phys. Rev. B **46**, 5047 (1992).
- <sup>10</sup>R. Bachmann *et al.*, Rev. Sci. Instrum. **43**, 205 (1972).
- <sup>11</sup>A. de Visser, Ph.D. thesis, University of Amsterdam, 1980.
- <sup>12</sup>A. Fert and P. M. Levy, Phys. Rev. B **36**, 1907 (1987).
- <sup>13</sup>A. Iandelli and A. Palenzona, J. Less-Common Met. **29**, 293 (1972).
- <sup>14</sup>N. E. Bickers, D. L. Cox, and J. W. Wilkins, Phys. Rev. B **36**, 2036 (1987).
- <sup>15</sup>I. Felner and I. Nowik, Phys. Rev. B **33**, 617 (1986).
- <sup>16</sup>J. M. Lawrence and R. D. Parks, in *Valence Instabilities and Related Narrow Band Phenomena*, edited by R. D. Parks (Plenum, New York, 1977), p. 443.
- <sup>17</sup>T. Naka *et al.*, Physica B **205**, 121 (1995).
- <sup>18</sup>T. E. Scott, in *Handbook on the Physics and Chemistry of Rare Earths* edited by K. A. Gschneidner, Jr. and L. Eyring (North-Holland, Amsterdam, 1978), Vol. 1, p. 591.
- <sup>19</sup>K. Kojima *et al.*, J. Magn. Magn. Mater. **140–144**, 1241 (1995); Y.-Y. Chen, J. D. Thompson, C. D. Immer, J. L. Sarrao, and Z. Fisk, unpublished results for single crystals.
- <sup>20</sup>G. Oomi *et al.*, J. Alloys Compd. **207–208**, 282 (1994).
- <sup>21</sup>R. A. Cowley, Phys. Rev. B **13**, 4877 (1976).
- <sup>22</sup>K. Takegahara and T. Kasuya, J. Phys. Soc. Jpn. **59**, 3299 (1990).